

# Joint Torque Sensor Embedded in Harmonic Drive Using Order Tracking Method for Robotic Application

Byung-jin Jung, Byungchul Kim, Ja Choon Koo, Hyouk Ryeol Choi, and Hyungpil Moon

**Abstract**—The main contribution of this work is the low-cost joint torque measurement method using the harmonic drive characteristics. To measure the external torque, we use the strain measurement of the flexspline of the harmonic drive. The flexspline of the harmonic drive is deformed by the external torque as well as by the velocity reducing operation, which creates “torque ripple” on the strain signal from the flexspline. As the frequency characteristics of such torque ripple are strongly related with the joint speed, an order tracking technique is used to compensate the torque ripple. The re-sampling based order tracking data acquisition is used to re-arrange the torque ripple signal into the order signal which has independent frequency characteristic to the joint speed. Then, a simple notch filter easily cancels the torque ripple from the re-arranged signal. Our algorithm switches the signal source between the order tracking and the ordinary time-based acquisition to overcome the zero velocity condition. To overcome the lack of order information at the starting of the joint motion, we propose a back propagation method using trained order sampling data. The developed joint torque sensing method is applied to the harmonic drive reducer of a robot manipulator’s joint and experimentally evaluated for the torque measurement during the motion of 5<sup>th</sup> order polynomial trajectory following.

**Index Terms**—Torque measurement, Notch filters, Filtering, Robot sensing systems

## I. INTRODUCTION

RECENTLY, robotic applications are extended to the human collaborative and dexterous force control areas from the conventional human-separated and position control based ones [1]–[3]. In this sense, not only the accurate position control but also the flexible reaction against the external disturbance is required for the robots to achieve the dexterity and the safety. Thus, the external force/torque sensing has become a vital part in many of force control required robotic applications [4]–[7].

The most intuitive way of torque sensing is the usage of the proportional relationship between the motor current and the motor torque. Unfortunately, most of robotic systems use the additional mechanical components that cause the unpredictable disturbance (e.g. friction) during the torque transfer from the motor to the robot link. The motor current based methods require the data analysis and accurate model estimation processes for the cancellation of such disturbances [8]. This process requires additional effort to the system development and the maintenance. On the other hand, conventional multi-axis force/torque sensors or joint torque sensors use special mechanical structures that are designed to transduce the external force/torque into the predictable deformation of themselves [9], [10].

Byung-jin Jung, is with Department of Mechanical Engineering, Sunkyunwan University and with Department of Intelligent Robotics Research Center of Korea Electronics Technology Institute, 25, Saenari-ro, Bundang-gu, Seongnam-si, Gyeonggi-do, Korea 13509, e-mail: jb-jin@keti.re.kr

Byungchul Kim is with Psylogic Inc., 806, U-Tower, Heungduk Central Road 120, Giheung-Gu, Yongin-City, Gyeonggi-Do, Korea, 446-908 e-mail: bckim@psylogic.com

Ja Choon Koo, Hyouk Ryeol Choi, and Hyungpil Moon are with Department of Mechanical Engineering, Sunkyunwan University, Chunchun-dong, Jangan-gu, Suwon, Gyeonggi-Do, Korea, 440-746 e-mail: {jckoo, hrchoi}@skku.edu, hyungpil@skku.edu (corresponding author)

The earlier work of this research was presented at 2014 IEEE Sensors.

Manuscript received July 10, 2016.

The complex shape of the structure itself increases the manufacturing cost of the joint torque sensor.

There are a few researches of developing a torque sensing method based on the strain measurement of the flexspline of harmonic drives [11]–[13]. The harmonic drive is a velocity transforming mechanical component, based on the strain wave gearing. Since it has the advantages of light weight, high reduction ratio in a small volume and weight, and extremely small backlash, the harmonic drive has become one of the widely used mechanical parts for the velocity reducer in a various robot joint systems [9], [16]. The components of the harmonic drive are illustrated in Fig. 1. The speed reducing operation of the harmonic drive is induced by the deformation of the flexible transmission component that is called as ‘flexspline’, which is indicated by the blue line in Fig. 1 (b). The left-most one in Fig. 1 (b) is called as ‘wave generator’ and the other is called as ‘circular spline’. When the wave generator rotates, the flexspline is deformed due to the elliptical shape of the wave generator. The deformation of the flexspline induces the relative motion of gearing components between the flexspline and the circular spline.

The harmonic drive is normally assembled with an axis-aligning constraint for the robust joint operation. This constraint is achieved by the hardware component of the robot joint (e.g.: a cross roller bearing) [14]. As the axis aligning hardware constraint of the harmonic drive application prevents the deformation caused by force/torque components other than the axial torque, the crosstalk error is inherently compensated. However, in spite of the advantages, as the flexspline is deformed by not only external torque but also reducing operation itself, the strain measurement signal is corrupted by the noise from reducing deformation. This phenomenon is called as ‘Torque ripple’ in this paper.

There are some of the ripple cancellation studies reported. The first well-known method is the hardware based ripple cancellation method. In this method, multiple measurement elements are aligned to cancel the ripple of each element [11], [12]. As the attempt to enhance the performance and productivity of torque sensing, the methods using a transparent film for alignment, a bridge circuit modification and gain tuning based signal compensation are reported [15]. Moreover, the switching algorithm using a set of multiple notch filters that have partially separated cutoff frequencies is introduced in [17] and Kalman filtering algorithm, using the state model of the torque ripple, is introduced in [13].

In this paper, we propose a robust torque sensing method by means of measuring the strain at the flexspline of harmonic drive, unlike conventional torque sensors which use an extra intermediate complaint structure between the driving unit (electric motor and gear train) and the output link. We suggest a new signal processing method for the compensation of the torque ripple. Though the raw strain signal is obtained from the strain gauges on flexspline same as other related previous researches such as [11], [12], [15], the performance of the sensing accuracy is not affected by the sensor alignment error. Furthermore, the continuity of measurement is not deteriorated by the supposed order tracking based torque measurement method. Moreover, in this paper, the authors discuss the condition that the order sampling cannot be triggered. The methods of source switching

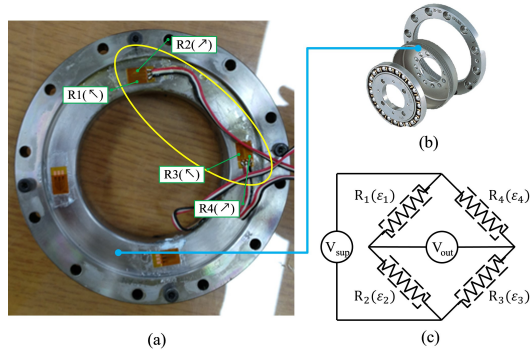


Fig. 1. Strain gauge attachment on harmonic drive. (a) Hardware overview, (b) Flex spline part, (c) Circuit composition

and back propagation are used as the solution for the zero velocity and re-acceleration condition. The developed method is experimentally compared with the current based torque measurement method. Experimental results show that the order tracking based harmonic drive embedded in torque sensor successfully measures the external torque without any complex model and filtering algorithm or high accuracies that conventional methods require.

The remaining of the paper is organized as follows. The section II discusses the hardware setting and torque ripple characteristics. In section III, we introduce the concept and the implementation issues of filtering method based on the order tracking analysis for torque ripple reduction. The section IV describes the experimental evaluation of the algorithm and we provide conclusion in section V.

## II. PROBLEM DESCRIPTION

### A. Hardware Setup

The flex spline of the harmonic drive in the robot joint experiences the radial and tangential strains during the operation. The tangential strain is mainly generated by the joint torque and the radial strain by reducing operation. The basic concept of the harmonic drive embedded joint torque sensing is to extract the tangential strain from the measurement signal mixed with the influence of the radial strain. A torque sensing element which is composed of two strain gauges in perpendicular directions is used to measure the tangential and radial strain of harmonic drive. The strain on diaphragm parts shows a sinusoidal curve which is convenient to analyze the frequency characteristics [11], [12]. The strain gauges are attached to the location of the red circles in Fig. 1 (a). At the same time, the strain gauge sensors are aligned approximately at  $45^\circ$  and  $135^\circ$  from the radial direction. This attachment condition is indicated by the arrows displayed in Fig. 1 (a). The yellow oval specifies the group of four strain gauges used in this paper. These four strain gauge sensors form a Wheatstone bridge circuit for the strain measurement of the flexspline as depicted in Fig. 1 (c).

As the flexspline is fixed on the outer structure of the harmonic drive, the deformation of the inner side is larger than the outer side. Because of the perpendicular alignment of the strain gauge, the tangential and the radial strain affecting on each sensing element show different characteristics. In each sensing element, the influence of the tangential strain is represented as compression at a strain gauge and extension at the other. Specifically, in Fig. 1 (a), the strain gauges notated with odd numbers are compressed while the strain gauges with even numbers are extended by the tangential strain. On the other hand, the influence of the radial strain is represented in the

same direction at the two strain gauges in each sensing element. This relationship can be described as follows.

$$\begin{aligned} \epsilon_1 &= (\epsilon_{t12} + e_{t1}) + \epsilon_{r12} + e_{r1} \\ \epsilon_2 &= -(\epsilon_{t12} + e_{t2}) + \epsilon_{r12} + e_{r2} \\ \epsilon_3 &= (\epsilon_{t34} + e_{t3}) + \epsilon_{r34} + e_{r3} \\ \epsilon_4 &= -(\epsilon_{t34} + e_{t4}) + \epsilon_{r34} + e_{r4}, \end{aligned} \quad (1)$$

where  $\epsilon_{tij}$  and  $\epsilon_{rij}$  stand for the influence of tangential and radial strain at the sensing element composed of strain gauge  $i$  and  $j$ . The variable,  $\epsilon_i$ , means the strain measurement value of each strain gauge. If all strain gauges are well-aligned exactly at the direction of  $45^\circ$  and  $135^\circ$  from the radial direction, the amount of the influence of the tangential and the radial strain at the strain gauges of a sensing elements are identical. However, the unknown errors ( $e_{ti}$  and  $e_{ri}$ ) exist in the relationship. The relation between the supply voltage and the output voltage of the Wheatstone bridge circuit composed with these strain gauges can be described as follows.

$$V_{out} = \frac{K_{full}}{4} (\epsilon_1 - \epsilon_2 + \epsilon_3 - \epsilon_4) V_{sup}, \quad (2)$$

where  $V_{out}$  means the output voltage of measurement,  $V_{sup}$  means the supply voltage of the circuit, and  $K_{full}$  represents the gain of the bridge circuit. If the alignment of the sensing element is perfect, only the mean value of the influence of the tangential strain affects the output. However, in general, the unknown errors caused by the imperfect alignment affect to the output. When we substitute (1) in (2), we obtain the following.

$$V_{out} = V_t + V_r, \quad (3)$$

where

$$V_t = \frac{K_{full}}{4} (2\epsilon_{t12} + 2\epsilon_{t34} + \Delta_t) V_{sup} \quad (4)$$

$$V_r = \frac{K_{full}}{4} (\Delta_r) V_{sup} \quad (5)$$

The variables  $V_t$  and  $V_r$  mean the voltage output influenced by the tangential and the radial strain, respectively. Moreover,  $\Delta_t$  and  $\Delta_r$  mean the overall error in the tangential and the radial strain, respectively.

The error term,  $\Delta_t$  in (4) is independent of the joint velocity and has constant characteristics unless the attachment condition of the strain gauge is changed. This error is automatically compensated during the initial calibration process of finding the joint torque gain value. However,  $\Delta_r$  does not have the constant characteristic and varies by the position of the wave generator. The effect of  $\Delta_r$  remains in the measurement output as (5). This effect is represented as the fluctuation of the output signal that hinders the accurate joint torque measurement. In the following subsection, the frequency characteristics of the torque ripple are analyzed.

### B. Torque Ripple Characteristics

The speed reduction of the harmonic drive is operated with the rotation of the elliptical-shaped wave generator. The radial strain of the flex spline is caused by the difference of the major and minor axis lengths of the wave generator. Therefore, the frequency characteristics of the radial strain and the torque ripple depend on the speed of the wave generator. For the study of the torque ripple, we analyze the frequency of the torque ripple at various input velocities. This relationship is shown in the upper part of Fig. 2. The  $x$ (horizontal),  $y$ (vertical) and  $z$ (depth) axes of each graph mean the frequency/order, the amplitude of the frequency/order component of the signal, and the velocity of the wave generator.

There are significantly dominant frequency components shown in Fig. 2 and the dominant frequencies of the output signal vary by the

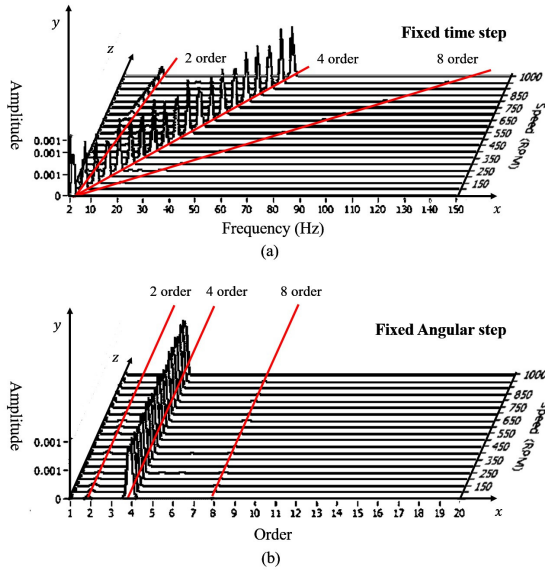


Fig. 2. Effect of the re-sampling based order tracking. (a) Fixed time step, (b) Fixed angular step

velocity level of the wave generator. Specifically, the signals with 2, 4 and 8 times of the harmonic drive input speed dominantly appear in the frequency of the torque ripple. Moreover, the largest amplitude of the frequency component is shown at a special frequency band which is 4 times of the rotation speed. This phenomenon is caused by the composition of 2 sensing elements and the elliptical shape of the wave generator that has 2 major and minor axes. The other dominant frequencies can be considered as the harmonic frequency of the flexspline vibration caused by the wave generator.

As this result represents, the harmonic drive input speed has a proportional relationship with the frequency characteristics of the torque ripple. In the case of robotic applications, the joint velocity varies for desired force/position trajectories. This means that the torque ripple has various and changing frequency characteristics during the robot operation and cannot be canceled with a simple digital filter with a fixed cutoff frequency only. Because of this reason, a special signal processing method that can eliminate the constantly changing characteristics of the torque ripple signal is required.

### III. THEORETICAL BACKGROUND AND APPLICATION

An initial work of the torque measurement using order filters is presented in [21]. In this section, we summarize the main idea of the order filter for the sake of better readability. As a new contribution of this work, the performance decreasing condition of the order analysis in robotic applications is discussed, and in the following subsection, we suggest the solution to these practical issues.

#### A. Re-sampling Based Order Tracking

As the torque ripple is generated by the strain gauge attachment error, the ripple signal may have inconsistent amplitudes in device by device. Although the frequency of the torque ripple varies by the speed of the wave generator, it is discussed in Sec. II that the relationship itself between the ripple frequency and the wave generator velocity is constant. In this reason, we use the order tracking method for the torque ripple cancellation. The order tracking is a well-known signal processing method in the field of rotating machinery. The expression ‘order’ is a term that represents the relationship between the frequency of the output signal and the input

rotation speed in the multiple numbers. The order tracking is a process that re-arrange the output signal with the frequency scale which is proportional to the input rotation speed [11], [12]. In General, the input rotation speed is considered as the reference speed/frequency. If a signal has the same frequency as the reference speed, the frequency is called as ‘order 1’. In other words, the order characteristic of a signal means the number of the rotational signal for the one full input rotation. For example, if a signal has the order 4 (frequency same as 4 times of the reference signal), the result of order tracking has a shape of 4 crests and valleys for the period of one rotation. Even if the frequency of the original signal is varied, the frequency of the re-arranged signal is conserved by the constant relationship between the reference speed and the signal frequency itself. Because of this characteristic of the order tracking, the simple fixed frequency filters can be applied. Fortunately, the torque ripple is generated by the rotational input (from the wave generator) and the frequency characteristics have a constant relationship with the input speed.

There are various ways of realizing the order tracking in rotating machinery field [18], [19]. Among them, the re-sampling based order tracking method can be enabled with a high-frequency data acquisition device and the accurate position measurement [20]. The main idea of re-sampling based order tracking is the ‘location based data acquisition’. In other words, to re-arrange the signal with the scale of the reference frequency, the signal is acquired at the fixed location, not at a constant time intervals. Originally, the re-sampling position of the rotation shaft is calculated from the rotational velocity in each time step as discussed in [18]. Fortunately, the robotic joints provide position information in high resolution from the encoder for the accurate position control and we use the position information directly for the re-sampling of the ripple data. Specifically, the encoder measures the rotation of the motor shaft attached to the wave generator. The sensing points are configured as 2500 fixed positions around the motor shaft. Meanwhile, the data acquisition device measures the  $V_{out}$  data with high frequency and receives the position data from the encoder. When the rotating shaft passes each sensing point, the data acquisition device gathers the strain data at sensing position and re-arranges them in the form of the order tracking signal.

Referenced from [20], the coefficients of sine and cosine terms in Fourier Transform of the re-arranged signal on the angle domain can be described as (6).

$$\begin{aligned} a_n &= \frac{1}{N} \sum_{n=1}^N x(n\delta\theta) \cos(2\pi o_n \delta\theta) \\ b_n &= \frac{1}{N} \sum_{n=1}^N x(n\delta\theta) \sin(2\pi o_n \delta\theta) \end{aligned} \quad (6)$$

The terms of  $a_n$  and  $b_n$  are the Fourier coefficients of the cosine and sine terms respectively for order  $o_n$ . The variable  $y(n\delta\theta)$  is the torque ripple signal at  $n^{th}$  sample,  $N$  is the total number of time points over which the transform is performed and  $\delta\theta$  represents the angular step of the data acquisition. In the result, the order characteristics of re-sampled data in (6) only depend on the position, therefore it is independent of velocity variations.

The effect of the re-sampling based order tracking method is shown in the lower part of Fig. 2. As discussed in Sec. II, Fig. 2 (a) represents the frequency characteristics of the raw torque ripple signal which has the frequency dependency on the joint speed. In contrast, the frequency characteristics of the re-sampled torque ripple are independent of the velocity change of the wave generator as shown in Fig. 2 (b).

Due to the re-sampling based order tracking, the torque ripple is re-arranged at fixed dominant frequencies of  $2^n$  order. The torque ripple of the re-arranged signal can be conveniently canceled by a

set of simple fixed notch filters. The discrete notch filters with 2, 4 and 8 order of cutoff frequency are applied to reduce the torque ripple and the filtered signal is re-converted to the time-based signal with synchronized output timing to represent the joint torque.

### B. Dead Zone in Order Filtering

The order tracking method is originally developed for continuous operations of a rotational joint at non-zero speeds. As the re-sampling of the strain data is triggered by the change of the joint position, the order tracking method used in this paper cannot generate the order tracking signal in case of the zero velocity condition of the input. Unfortunately, robot systems frequently face the zero velocity condition during operations. (e.g: the static force interaction or the directional change of the joint motion.) We call the condition which cannot generate the order signal as ‘dead zone’.

To solve this problem, the data acquisition algorithm is designed to switch the signal acquisition source from the order signal to the raw signal. As the characteristic of torque ripple has the proportional relationship with the joint speed, the torque ripple effect on the strain gauge measurement disappears when the joint speed is zero. Because of the characteristics, the lack of the order tracking signal can be covered with the raw strain gauge signal for the zero velocity condition. However, the effect of the torque ripple in the raw signal still remains as the offset error from the order tracking signal after the source switching. As the torque ripple is not newly generated during the zero speed, the offset is conserved till the joint begins the motion again. In this reason, the offset can be simply compensated by the subtraction of the initial offset from the raw signal. Practically, the data acquisition device calculates the offset when the joint speed is measured to be zero and the calculated offset is used to compensate the raw signal when the joint remains as a stop motion.

When the joint begins the motion after the zero speed condition, the signal acquisition source is switched back to the order tracking. At this moment, the order tracking signal does not contain full information of the order characteristic unless one full revolution of the wave generator is achieved. This means that the filter tends to show a dull filtering performance caused by the lack of the order information at the beginning of acceleration from a stop. This problem can be overcome by the back propagation of the order signal information. For the back propagation, the re-sampled data is stored in a buffer and updated during the motion with a length which is enough to represent the entire order information of the joint revolution. The update process stops and conserves the order information data when the joint remains in the zero velocity condition. When the joint restarts the motion, the saved data is collated in the ‘back’ of the newly re-sampled order tracking signal to recover the lost order information before the zero speed condition. As the stored data contains sufficient order information for the filtering, the order filter is able to maintain the performance during the re-starting condition.

## IV. EXPERIMENTS AND RESULTS

### A. Experiment System Setup

The experiment is conducted with a robotic manipulator whose joints contain harmonic drives as illustrated in Fig. 3. We use SHD-25 of Harmonic Drive Inc. and the strain gauge is attached to the outer diaphragm part of the flexspline as shown in Fig. 1 (a), which has a hat-like flexspline different from the cup-like shape of flexspline used in [11]. The diaphragm part suffers lower torque ripples than the cylindrical part. Specifically, the ripple on the cylindrical part is induced by the wave generator directly but the affection of the wave generator transferred to diaphragm part indirectly via cylindrical part. In this reason, the diaphragm part is the most suitable part for the

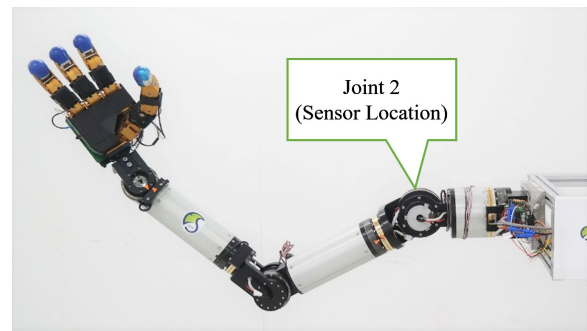


Fig. 3. Experimental environment.

strain gauge attachment as discussed in [11]. However, the diaphragm part of both types has an equivalent characteristic in terms of torque sensing. This deformation characteristic of flexspline only depends on the connection type (direct or indirect) of the local part and the wave generator. In other words, the torque ripple characteristic is not so sensitive to the specific location of the diaphragm part – inside (cup-like) or outside (hat-like) of the cylindrical part. Moreover, it is noted that the performance of our torque measurement method is independent of the variation of the strain gauge attachment such as the number of strain gauges, wiring types, or the locations of strain gauges. Our torque sensing method can be applicable to both of cup-like and hat-like flexsplines.

The robot joint is controlled by Gold Solo whistle 20/100EE motion controller of Elmo Inc. The position of the motor shaft is measured with a quadratic incremental encoder of US digital. For the realization of the order analysis, we use compactRIO series of the National Instrument Inc., the high-speed FPGA device for the data acquisition, re-sampling and notch filter processing.

The signal from the strain gauge and the encoder is connected to FPGA device for the order tracking. The FPGA device measures the strain signal constantly during the entire operation in 40MHz of frequency. The re-sampling process is triggered by the change of encoder signal. In this tracking process, 2500 positions on a single revolution of the motor are used to re-sampling trigger. In the result of the order tracking, the frequency normalized signal is generated. The resulting signal of the order tracking accomplishes the fixed frequency characteristics independent of the joint speed, which is filtered by the notch filters with fixed frequency windows.

At the same time, the time difference between the triggers is measured in  $\mu sec$  to calculate the velocity in every triggering position. When the triggering is not activated during  $1\mu sec$ , the controller switches the output of the measurement from the stopped order signal to the raw signal that does not contain torque ripple due to the zero speed condition. The controller calculates the difference between the filtered signal and the raw signal and compensates the offset caused by the ripple on the raw signal.

### B. External Torque Measurement Experiment

The robotic manipulator follows the trajectory described at Fig. 4. The motion is started at  $0.16sec$  and finished at  $3.79sec$ , emphasized with black dashed vertical line at the start and the end point in Fig. 4. The raw signal and the order tracking based ripple filter applied signal are plotted in Fig. 5. The blue line in Fig. 5 is the raw signal and the red line is the order filtered signal. Thus, the red line in Fig. 5 represents the amplitude of torque ripple which is reduced by the order tracking based compensation.

For the performance evaluation, the desired joint torque trajectory and current based torque measurement data are prepared. The errors



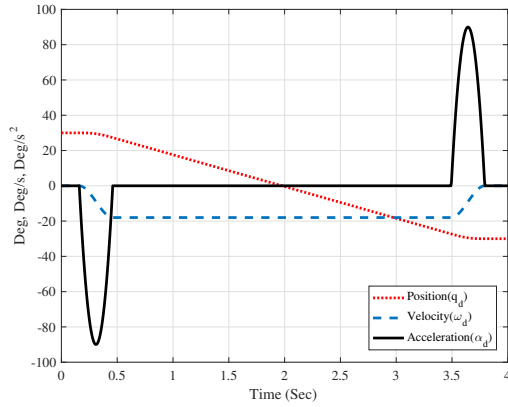


Fig. 4. Trajectory for External torque measurement experiment. Desired position(Dotted red,  $q_d$ ), velocity(Dashed blue,  $\omega_d$ ), acceleration(Solid black,  $\alpha_d$ )

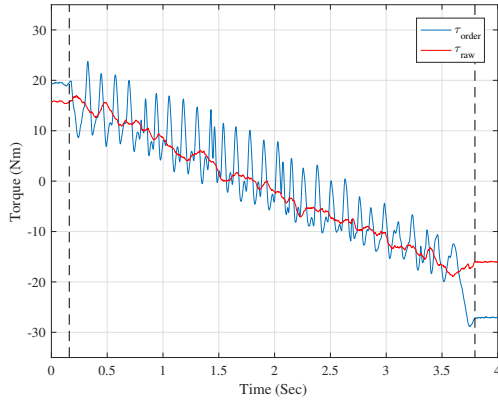


Fig. 5. Ripple and offset compensation results

between the measured torques (current based, order filtering based) and the desired output torque trajectory are compared for evaluation. The current based torque measurement contains the friction compensation based on the conventional exponential model [22] and the low-pass filter like conventional methods. The low-pass filter with  $130\text{Hz}$  of the cutoff frequency is applied for conditioning of the friction-compensated current signal.

The desired joint torque ( $\tau_d$ ) can be described with the model of the inertial force and the gravity as follows.

$$\tau_d = M(q_d)\alpha_d + G(q_d), \quad (7)$$

where  $\alpha_d$  is the desired acceleration and obtained from the pre-planned joint trajectory as depicted in Fig. 4.  $M(q_d)$  and  $G(q_d)$  are the model of the inertia and the gravity applied to the link, respectively, when the joint position has the desired value of  $q_d$ . In the result, the measured torque data and the desired torque data are displayed in Fig. 6. The magenta-dashed line is the current based measured torque, the solid line is the result of the developed method and the thick dashed black line represents the reference desired torque calculated from the model in (7).

The current based torque measurement still suffers from several uncertainties and noises even after the friction compensation and signal filtering. The harmonic drive friction is affected by the temperature and the condition of lubricant. The friction compensation error caused by these nonlinear characteristics remains in the result. Moreover, the

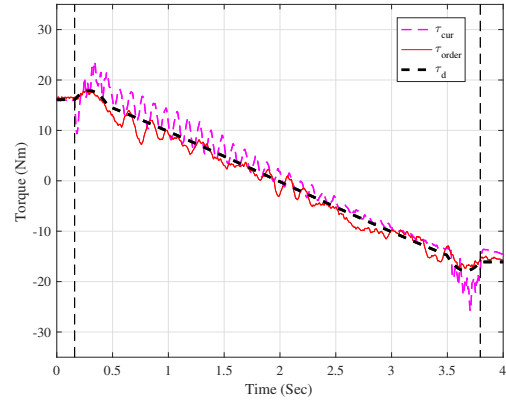


Fig. 6. External torque measurement results

TABLE I  
RESULT OF THE TORQUE MEASUREMENT

	$\tau_{\text{cur}}$	$\tau_{\text{order}}$	$\frac{\tau_{\text{order}}}{\tau_{\text{cur}}}$
Error <sub>max</sub>	8.2Nm	4.8Nm	58%
Error <sub>RMS</sub>	1.4Nm	0.9Nm	64%

wave generator alignment error can be influential to the additional load of motors. The assembly condition of the joint module causes uneven operational torque on the revolution of the joint module [23], [24]. The frequency of this effect also has a linear relationship with the joint speed like the torque ripple. Additionally, the noise caused by the motor controller characteristic can be also influential to the performance. These uncertainties are the main drawbacks of current based torque measurement. However, the effect of these factors is hard to be cleared in conventional robotic systems.

The Root Mean Square (RMS) value of the error between the model and the measurement torque at the entire trajectory is listed in Table I. The current based measurement ( $\tau_{\text{cur}}$ ) has 8.2Nm of maximum error and 1.4Nm of RMS error during the motion. On the other hand, the torque sensor based on the order tracking and filtering ( $\tau_{\text{order}}$ ) shows more accurate results which are 4.8Nm of maximum error and 0.9Nm of RMS error. The torque error measured from the proposed method shows 58% of the error measured by the current based method in its maximum error and 64% in RMS error, respectively.

## V. CONCLUSION

The torque ripple filtering algorithm based on the order tracking analysis for harmonic drives is discussed and experimentally evaluated in this paper. The re-sampling based order tracking method is used to normalize the frequency characteristics of the torque ripple. As the re-sampling order tracking method re-arranges the sampling signal referenced with input speed, the frequency characteristics of the output signal do not change under input speed variations. A notch filter which has a fixed cutoff range is used to filter out the torque ripple from the raw strain signal.

For the practical application, the compensation method for the performance degradations near zero velocity is considered. As the re-sampling is triggered by position changes, the order tracking cannot produce sufficient order information for the torque measurement and the ripple filtering at zero velocity. To solve this problem, the signal switching and back propagation algorithm is introduced

to conserve order information for the zero velocity and the re-acceleration condition.

The experiment is performed on a robot manipulator with the harmonic drives as the joint reducer. The performance of the torque ripple filtering method based on the order tracking analysis is compared with the current based torque measurement method. In the result, the output signal of the suggested measurement method reports lower error rates. Moreover, the developed algorithm guarantees continuous torque measurement in various velocity conditions without an accurate ripple model.

#### ACKNOWLEDGMENT

This work supported by the Ministry of Trade & Energy (MOTIE) and the Korea Evaluation Institute of Industrial Technology (KEIT) with the program number of 10040210 and the National Research Foundation of Korea(NRF) grant funded by the Korea government(MSIP) (No. 2016R1A2B4010880)

#### REFERENCES

- [1] A. Pervez and J. Ryu, "Safe physical human robot interaction, past, present and future," *Journal of Mechanical Science and Technology*, vol. 22, no. 3, pp. 469-483, Mar., 2008.
- [2] O. Stasse, R. Ruland, F. Lamiraud, A. Kheddar, K. Yokoi and W. Prinz, "Integration of humanoid robots in collaborative working environment: a case study on motion generation," *Intelligent Service Robotics*, vol. 2, no. 3, pp. 153-160, Jul., 2009.
- [3] J. T. C. Tan, F. Duan, Y. Zhang, K. Watanabe, R. Kato and T. Arai, "Human-Robot Collaboration in Cellular Manufacturing: Design and Development," *Proc. of 2009 IEEE/RSJ International Conference on Intelligent Robots and Systems*, pp. 29-34, 2009.
- [4] F. Aghili, M. Buehler and Q. C. Ha, "Dynamics and Control of Direct-Drive Robots with Positive Joint Torque Feedback," *Proc. of 1997 IEEE International Conference on Robotics and Automation*, pp. 153-161, 1997.
- [5] A. D. Luca, A. Albu-Schaffer, S. Haddadin and G. Hirzinger, "Collision Detection and Safe Reaction with the DLR-III Lightweight Manipulator Arm," *Proc. of 2006 IEEE/RSJ International Conference on Intelligent Robots and Systems*, pp. 1623-1630, 2006.
- [6] S. Haddadin, A. Albu-Schaffer, A. D Luca and G. Hirzinger, "Collision detection and reaction: A contribution to safe physical Human-Robot Interaction," *Proc. of 2008 IEEE/RSJ International Conference on Intelligent Robots and Systems*, pp.3356-3363, 2008.
- [7] M. J. Kim, Y. J. Park, and W. K. Chung, "Design of a momentum-based disturbance observer for rigid and flexible joint robots," *Intelligent Service Robotics*, vol. 8, no. 1, pp. 57-65, 2015.
- [8] H. Olsson, K.J. Åström, C. C. Wit, M. Gäfvert and P. Lischinsky, "Friction models and friction compensation," *European journal of control*, vol. 4, no. 3, pp. 176-195, Jun., 1998.
- [9] G. Hirzinger, A. Albu-Schaffer, M. Hahnle, I. Schaefer, N. Sporer, "On a new generation of torque controlled light-weight robots," *Proc. of 2001 IEEE International Conference on Intelligent Robots and Systems*, pp. 3356-3363, 2001.
- [10] I. W. Park, J. Y. Kim, S. W. Park and J. H. Oh, "Development of humanoid robot platform khr-2 (kaist humanoid robot 2)," *International Journal of Humanoid Robotics*, vol. 2, no. 4, pp. 519-536, Dec., 2005.
- [11] M Hashimoto, Y. Kiyosawa, H Hirabayashi, R. P. Paul, "A joint torque sensing technique for robots with harmonic drives," *Proc. of 1991 IEEE International Conference on Robotics and Automation*, pp. 1034-1039, 1991.
- [12] M Hashimoto, T Shimono, K Koreyeda, H Tanaka, Y Koyosawa, H Hirabayashi, "Experimental study on torque control using harmonic drive built-in torque sensors," *Proc. of 1992 IEEE International Conference on Robotics and Automation*, pp.2026-2031, 1992.
- [13] H. D. Taghirad, A. Helmy, P. R. Bglanger, "Intelligent Built-in Torque Sensor for Harmonic Drive Systems," *IEEE Transactions on Instrumentation and Measurement*, vol. 48, no. 6, pp. 969-974, Dec., 1997.
- [14] A. Albu-Schäffer, S. Haddadin, C. Ott, A. Stemmer, T. Wimböck and G. Hirzinger, "The DLR lightweight robot: design and control concepts for robots in human environments," *Industrial Robot: An International Journal*, vol. 34, no. 5, pp. 376-385, 2007.
- [15] J. W. Sensinger and R. F. Weir, "Improved torque fidelity in harmonic drive sensors through the union of two existing strategies," *IEEE/ASME Transactions on Mechatronics*, vol. 11, no. 4, pp. 969-974, Aug., 2006.
- [16] D. Choi, S. Shin, J. C. Koo, H. R. Choi, and H Moon, "The SKKU hand: Work in progress," *Proc. of 2012 IEEE International Conference on Ubiquitous Robots and Ambient Intelligence*, pp. 437-438, 2012.
- [17] J. H. Kim, Y. L. Kim, and J. B. Song, "A switching notch filter for reducing the torque ripple caused by a harmonic drive in a joint torque sensor," *Transactions of the Korean Society of Mechanical Engineers*, vol. 35, no. 7, pp.709-715, Jul., 2011.
- [18] R. Potter and M. Gribler, "Computed order tracking obsoletes older methods," *SAE Technical Paper*, no. 891131, May, 1989.
- [19] E. D. S. Munck and K. R. Fyfe, "Computed order tracking applied to vibration analysis of rotating machinery," *Canadian Acoustics.*, vol. 19, no.4, pp. 57-58, Sep., 1991.
- [20] J. R. Blough, D. L. Brown and H. Vold, "The Time Variant Discrete Fourier Transform as an Order Tracking Method," *SAE Technical Paper*, No. 972006, May, 1997.
- [21] B. Jung, B. Kim, S. Kim, J. Koo, H. R. Choi and H. Moon, "Torque ripple compensation method for joint torque sensor embedded in harmonic drive using order analysis," *Proc. of IEEE Sensors 2014*, pp. 1932-1935, 2014.
- [22] H. Olsson, K.J. Åström, C. Canudas de Wit, M. Gäfvert and P. Lischinsky, "Friction models and friction compensation," *European journal of control*, vol. 4, no. 3, pp. 176-195, Dec., 1998.
- [23] C.W. Kennedy and J.P. Desai, "Estimation and modeling of the harmonic drive transmission in the Mitsubishi PA-10 robot arm," *Proc. of 2003 IEEE International Conference on Intelligent Robots and Systems*, pp. 3331-3336, 2003.
- [24] T.D. Tuttle, *Understanding and modeling the behavior of a harmonic drive gear transmission*, Massachusetts Institute of Technology Cambridge Artificial Intelligence Laboratory, No. AI-TR-1365, 1992.